

Improving Precision in Time-Gated FLIM for Low-Light Live-Cell Imaging

Ching-Wei Chang¹ and Mary-Ann Mycek^{1,2,3}

¹Department of Biomedical Engineering, University of Michigan, Ann Arbor, MI 48109-2099

²Comprehensive Cancer Center, University of Michigan, Ann Arbor, MI 48109-2099

³Applied Physics Program, University of Michigan, Ann Arbor, MI 48109-2099
mycek@umich.edu

Abstract: Minimizing stress to live-cell systems during imaging is critical. Time-gating optimization and image denoising were employed independently and in combination to significantly improve precision in low-light time-gated FLIM.

©2009 Optical Society of America

OCIS codes: (100.2000) Digital image processing; (170.6920) Time-resolved imaging.

1. Introduction

Fluorescence Lifetime Imaging Microscopy (FLIM) is a molecular imaging technique that is useful for biological studies in living cells and tissues [1, 2]. When high-intensity light sources such as lasers are used for fluorescence excitation, it is important to ensure that live-cell systems remain viable and do not become significantly stressed.

Error analysis helps to achieve precision in lifetime determination with low-light live-cell imaging [3-5]. We have combined error analysis and Monte Carlo simulations to develop a temporal approach to enhance the precision of time-gated FLIM. This approach can involve both optimal gating and curve fitting. We have compared the precision associated with various lifetime determination techniques, and then searched parameter space in order to find optimal gating conditions in terms of minimal achievable relative standard deviation. Precision and accuracy were investigated via Monte Carlo simulations that included Poisson noise. The results were validated with fluorescence lifetime standards and fluorescent beads.

Because time-gated FLIM produces images for each gating, another way to improve precision in low-light FLIM is to utilize spatial information from the gated images to remove noise. Total variation (TV) models are commonly used denoising algorithms [6, 7]. We have considered several TV denoising models to improve the precision of lifetime determination with low-light FLIM. These methods remove electronic-related noise from FLIM images and hence can increase the precision with which the lifetimes are determined.

Since the temporal and spatial methods apply to different dimensions, we assume that they work independently and their precision improvements are additive. We test this assumption when the pixel-to-pixel variation due to noise in one image is high enough to cause possible unexpected nonlinear effects. We demonstrate that the precision improvements from the temporal and spatial techniques are independent and additive in a regime pertinent to live-cell FLIM studies.

2. Methods

2.1. Fluorescence Lifetime Imaging Microscopy (FLIM)

Images were acquired with a time-domain FLIM system, the instrumentation of which has been described previously [8]. To implement time-gated FLIM, recently we have designed and characterized a novel time-domain,

wide-field FLIM system for picosecond time-resolved imaging for biological applications [9]. A dye laser pumped by a nitrogen laser for UV-visible-NIR excitation provides a wide-field, less expensive, and potentially portable alternative to multi-photon excitation for sub-nanosecond FLIM of biological specimens [9]. A sample is illuminated by an excitation pulse and the fluorescence emission is recorded by an intensified charge-coupled device (ICCD) camera at a gate delay controlled by the intensifier, with emission intensities integrated during a gate width. This system has a large temporal dynamic range (750 ps – 1 μ s), 50 ps lifetime discrimination, and spatial resolution of 1.4 μ m, which make it very suitable for studying a variety of endogenous and exogenous fluorophores in biological samples [10-12]. Fluorescence lifetime maps are determined by first acquiring fluorescence intensity images at four gate delays and then calculating the lifetime values from the intensity decay on a pixel-by-pixel basis (further described below).

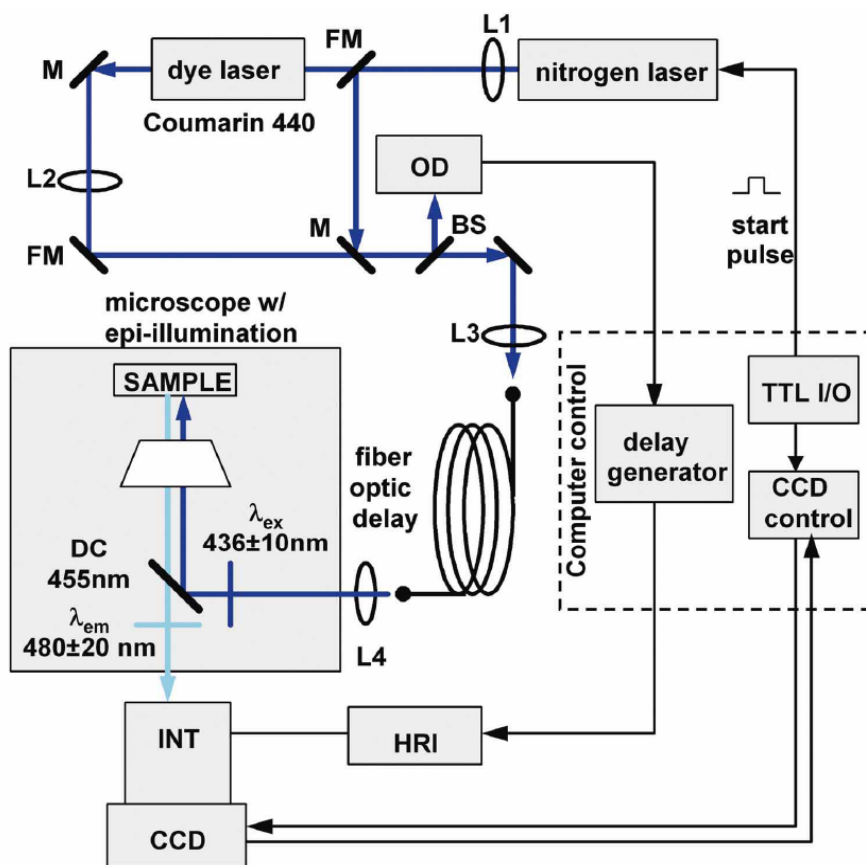


Figure 1 The time-gated FLIM setup used for this study. Abbreviations: CCD = charge-coupled device; HRI = high rate imager; INT = intensifier; TTL I/O = TTL input/output card; OD = optical discriminator; BS = beam splitter; DC = dichroic mirror; FM = “flippable” mirror; L1, L2, L3, L4 = quartz lenses; M = mirror. Thick solid lines = light path; thin solid line = electronic path. [8]

Figure 1 illustrates our FLIM system instrumentation, with some main experimental specifications for imaging living cells described below. The excitation source was composed of a pulsed nitrogen laser (GL-3300, Photon Technology International, Lawrenceville, NJ) pumping a dye laser (GL-301, Photon Technology International, Lawrenceville, NJ), with a wavelength range from UV through near infrared (NIR), depending on the dye in use. An

optical fiber (SFS600/660N, Fiberguide Industries, Stirling, NJ) was used to deliver the excitation light to a research-grade, inverted microscope (Axiovert S100 2TV, Zeiss, Germany) in epi-illumination mode. The optical fiber had the added benefit of homogenizing the spatial intensity distribution of the beam. A beam splitter split a reference pulse from the excitation light and sent it to an optical discriminator to generate an electronic pulse, which offered a time reference to a picosecond delay generator (DEL350, Becker & Hickl, Germany), whose output was then used for triggering the gated intensified CCD (ICCD) camera (Picostar HR, LaVision, Germany). The ICCD had variable intensifier gain and gate width settings varying from 200 ps to 10 ms and can be used to implement high-speed imaging in other applications as well [13].

2.2. Sample Preparation

Fluorescent beads with diameters of 10 μm (Polysciences, Warrington, PA) were suspended in distilled water to produce a solution with a final concentration of 1.5×10^6 beads/mL. Before imaging, 200 μL of the solution was placed on a delta T dish (Bioptechs, Butler, PA), and the imaging process was begun after the beads had settled to the bottom of the dish. All beads had excitation/emission maxima of 441/486 nm, as specified by the manufacturer. A 40 x microscope objective was used in the FLIM system.

2.3. Temporal Method to Improve Precision

In this study, single-exponential temporal optimization was utilized. The optimal gating was determined by Monte Carlo simulations, in which the relative standard deviation (RSD) was minimized by changing the gate width (g) and the time interval between two consecutive gates (dt), assuming that only Poisson noise was present. Since the intensity profile is $I(t) = \alpha \exp(-t/\tau)$, the RSD of either α (the pre-exponential term) or τ (the lifetime) could be minimized. As a first step, we investigated the variability in τ determination. With the sample mentioned above, the optimal gating was determined to be around $dt = 2.5$ ns and $g = 10$ ns.

2.4. Spatial Method to Improve Precision

TV models are constructed with the definition of their “energy”, through minimization of which the processed image (symbolized as “ u ”) evolves to a stable state that should be close to the original image without noise corruption. The basic form of the “energy” includes a regularization term, which utilizes total variation (defined as the integral of the absolute value of the gradient of the image, assuming the image is a continuous function) to denoise the input image (symbolized as “ f ”), and a fidelity term, which implements fitting of the processed image to the input image and decides how large the “distance” can be between these two images. A favorable property of TV models is that they perform selective smoothing and hence, are edge-preserving.

The TV model we developed in this study, here denoted as f -weighted TV (FWTV), is based on an f -weighted fidelity term. According to our previous results, this TV model was chosen because it can deal with Poisson-distributed noise, as well as other forms of noise, with high flexibility and speed.

2.5. Lifetime Determination

To creating fluorescence lifetime maps rapidly, a four-gate protocol with a linearized least squares lifetime determination method is used on a pixel-by-pixel basis [4, 14, 15]:

$$\tau_p = - \frac{N(\sum t_i^2) - (\sum t_i)^2}{N \sum t_i \ln I_{i,p} - (\sum t_i)(\sum \ln I_{i,p})}$$

where τ_p is the lifetime of pixel p , $I_{i,p}$ is the intensity of pixel p in image i , t_i is the gate delay of image i , and N is the number of images. All sums are over i .

Additional steps in data processing are needed for more accurate lifetime map production. Before lifetime calculation, the step “background subtraction” takes average of the intensities of pixels within a specified background region and subtracts that average value from all pixels. Also, the step “reject” sets intensities to zero for all pixels with intensities below a certain value (assigned as the parameter “reject”) after background subtraction. After lifetime calculation, the step “tau range” sets lifetime to zero for all pixels with lifetime above a certain value (assigned as the parameter “taurange”) after lifetime calculation, to remove lifetime values in physically meaningless regions. In this study, “reject” was set to zero for better noise estimation and “taurange” was set to 15.

3. Results

3.1. Temporal Method

We were able to find the optimal gating for all practical parameter combinations with several lifetime determination approaches. The data can be represented with vector plots, in which minimally achievable RSDs and the g and dt values needed to achieve them can be presented in one single plot. We chose a subset of the results to validate, and these results agreed with measurements on lifetime standards with RSD differences as low as only $\sim 3\%$ (data not shown). The simulation and experimental results showed the same trend of RSD values versus other parameters.

3.2. Spatial Method

With live-cell images, FWTV can improve precision of local lifetime determination without significantly altering the global mean lifetime values. This result was demonstrated in an experiment where the denoising model was applied to images of living cells transfected with fluorescent proteins. This study utilized four gates of width 1.0 ns, and an interval of 0.2 ns between each pair of consecutive gates. The results (data not shown) indicated that after FWTV denoising, there was a notable improvement in the mean R^2 (from 0.8960 to 0.9508) and χ^2 (from 0.8956 to 0.3559) values, and hence, the precision associated with local lifetime determination. In addition, the mean lifetime and pre-exponential terms were not significantly affected by the denoising algorithm. These favorable results were attributed to the flexibility of the FWTV weightings, which can take into account additional ICCD errors that only exist in real images.

3.3. Combination of Temporal and Spatial Methods

The spatial approach and the temporal approach both improve the FLIM precision and they work independently. This is demonstrated in Figure 2, where the noise distribution within the fluorescent beads is illustrated. Note that this is an extremely low-light case with total photon counts only around 100. The holes inside the fluorescent beads (Figure 2 (a)) came from one of the lifetime calculation steps in which the τ values above a certain threshold were set to zero. Since this threshold was set to $\tau = 15$ ns, random fluctuation within the low-light images caused some pixels to have lifetime values more than three times larger than the expected values if the gating scheme was not optimal. After denoising (Figure 2 (c)), the image became smoother and the RSD value dropped, but the extremely high τ values above the threshold still could not be removed. Optimal gating (Figure 2 (b)) removed these artifacts and further decreased the RSD value, as well as reducing the diameter of the beads so that it became closer to the actual bead size of 10 μm . Further improvement was then achieved by denoising the optimally-gated image (Figure 2 (d)). A comparison of Figure 2 (b) and Figure 2 (d) shows that most of the remaining lifetime variations within the

beads in the optimally-gated image could be removed by denoising. Here, the combination of the temporal and spatial techniques resulted in about a five-fold improvement in precision. In addition, the results in Figure 2 suggest that the improvement from the spatial method (~7 % in this case) is independent of that from the temporal method (~32 % in this case).

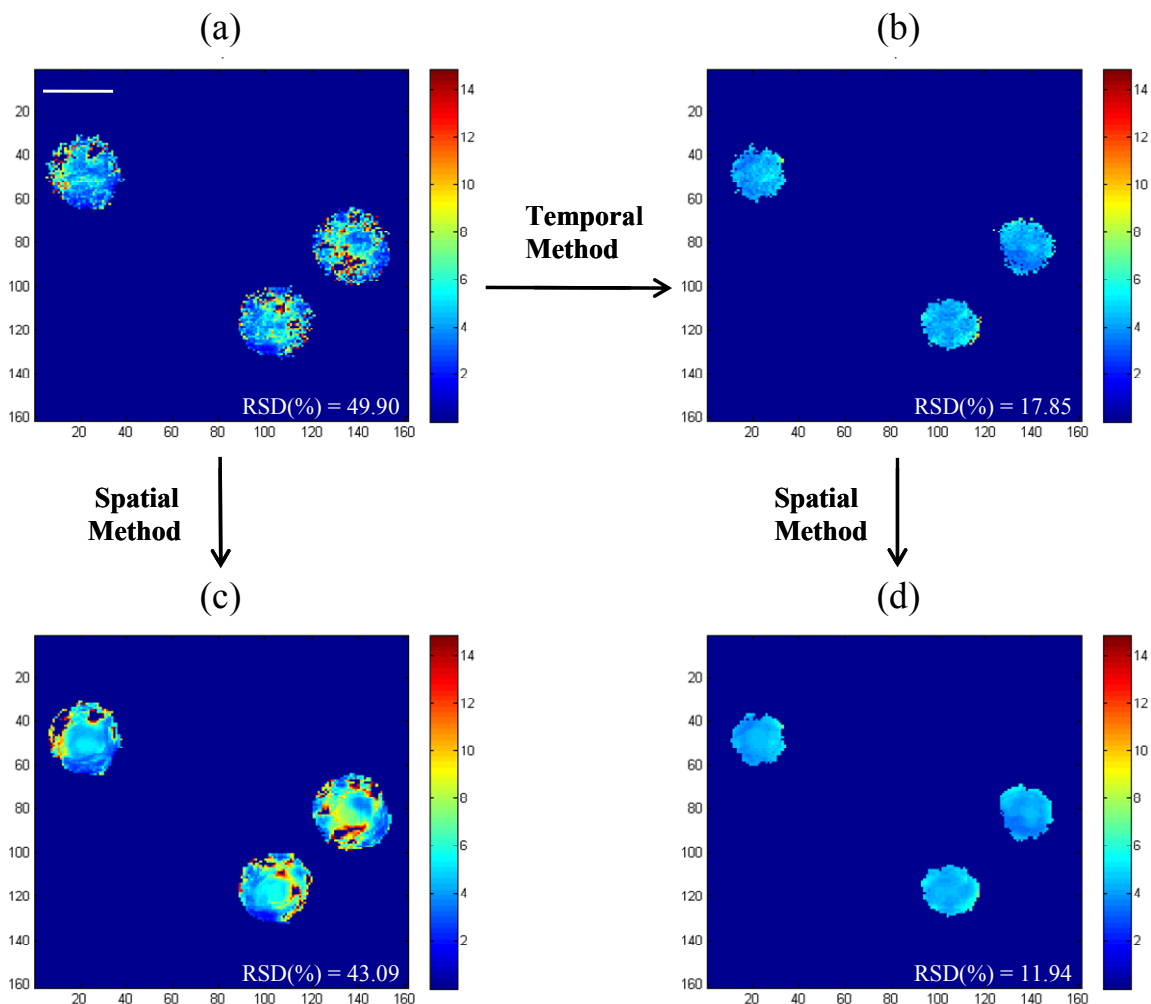


Figure 2 FLIM images of fluorescent beads acquired with a gate width of 10 ns and various values of the time interval dt between two gates: (a) $dt = 0.5$ ns, undenoised; (b) $dt = 2.5$ ns (optimal), undenoised; (c) $dt = 0.5$ ns, FWTV-denoised; (d) $dt = 2.5$ ns (optimal), FWTV-denoised. The improvements in precision from temporal method (~32% of RSD decrease) and spatial methods (~7% of RSD decrease) are additive and both easily observable in this extremely low-light case (total photon counts is around 100). The labeled RSD values were obtained from all non-zero pixels in the images. Scale bar: 15 μm .

We conclude that the temporal and spatial methods can be employed either independently or in combination to improve precision in low-light time-gated FLIM. When the two methods are combined, their notable five-fold (from 49.90% to 11.94%) improvements in precision are shown to be additive in our extremely low-light example (Figure 2).

4. References

1. Chang, C.W., D. Sud, and M.A. Mycek, *Fluorescence lifetime imaging microscopy*. Methods Cell Biol, 2007. **81**: p. 495-524.
2. Lakowicz, J.R., *Principles of fluorescence spectroscopy*. 2nd ed. 2004: Springer.
3. Ballew, R.M. and J.N. Demas, *An error analysis of the rapid lifetime determination method for the evaluation of single exponential decays*. Analytical Chemistry, 1989. **61**(1): p. 30-33.
4. Sharman, K.K., A. Periasamy, H. Ashworth, J.N. Demas, and N.H. Snow, *Error analysis of the rapid lifetime determination method for double-exponential decays and new windowing schemes*. Analytical Chemistry, 1999. **71**(5): p. 947-952.
5. Waters, P.D. and D.H. Burns, *Optimized gated detection for lifetime measurement over a wide-range of single exponential decays*. Applied Spectroscopy, 1993. **47**(1): p. 111-115.
6. Osher, S., M. Burger, D. Goldfarb, J.J. Xu, and W.T. Yin, *An iterative regularization method for total variation-based image restoration*. Multiscale Modeling & Simulation, 2005. **4**(2): p. 460-489.
7. Tadmor, E., S. Nezzar, and L. Vese, *A multiscale image representation using hierarchical (BV, L2) decompositions*. Multiscale Modeling & Simulation, 2004. **2**(4): p. 554-579.
8. Zhong, W., M. Wu, C.W. Chang, K.A. Merrick, S.D. Merajver, and M.A. Mycek, *Picosecond-resolution fluorescence lifetime imaging microscopy: a useful tool for sensing molecular interactions in vivo via FRET*. Optics Express, 2007. **15**(26): p. 18220-18235.
9. Urayama, P., W. Zhong, J.A. Beamish, F.K. Minn, R.D. Sloboda, K.H. Dragnev, E. Dmitrovsky, and M.A. Mycek, *A UV-visible-NIR fluorescence lifetime imaging microscope for laser-based biological sensing with picosecond resolution*. Applied Physics B-Lasers and Optics, 2003. **76**(5): p. 483-496.
10. Urayama, P.K., J.A. Beamish, F.K. Minn, E.A. Hamon, and M.-A. Mycek. *A UV fluorescence lifetime imaging microscope to probe endogenous cellular fluorescence*. in *Conference on Lasers and Electro-Optics*. 2002: Optical Society of America, Washington D.C.
11. Urayama, P.K. and M.A. Mycek, *Fluorescence lifetime imaging microscopy of endogenous biological fluorescence*, in *Handbook of Biomedical Fluorescence*, M.A. Mycek and B.W. Pogue, Editors. 2003, Marcel Dekker, Inc.: New York.
12. Zhong, W., P. Urayama, and M.-A. Mycek, *Imaging fluorescence lifetime modulation of a ruthenium-based dye in living cells: the potential for oxygen sensing*. Journal of Physics D: Applied Physics, 2003. **36**(14): p. 1689-1695.
13. Xu, Z., M. Raghavan, T.L. Hall, C.W. Chang, M.A. Mycek, J.B. Fowlkes, and C.A. Cain, *High speed imaging of bubble clouds generated in pulsed ultrasound cavitation therapy-histotripsy*. Ieee Transactions on Ultrasonics Ferroelectrics and Frequency Control, 2007. **54**(10): p. 2091-2101.
14. Bugiel, I., K. König, and H. Wabnitz, *Investigation of cell by fluorescence laser scanning microscopy with subnanosecond time resolution*. Lasers in the Life Sciences, 1989. **3**(1): p. 47-53.
15. Wang, X.F., T. Uchida, D.M. Coleman, and S. Minami, *A two-dimensional fluorescence lifetime imaging system using a gated image intensifier*. Applied Spectroscopy, 1991. **45**(3): p. 360-366.